Title

Audibility, speech perception and processing of temporal cues in ribbon synaptic disorders due to OTOF mutations

Journal

Hearing Research, 330(Pt B)

ISSN

0378-5955

Authors

Santarelli, Rosamaria
del Castillo, Ignacio
Cama, Elona
et al.

Publication Date

2015-12-01

DOI

10.1016/j.heares.2015.07.007

Hearing Research 330 (2015) 200–212

Contents lists available at ScienceDirect

Hearing Research

journal homepage: www.elsevier.com/locate/heares

Review

Audibility, speech perception and processing of temporal cues in ribbon synaptic disorders due to *OTOF* mutations

Rosamaria Santarelli [a, b, *], Ignacio del Castillo [c, d], Elona Cama [a, b], Pietro Scimemi [a, b], Arnold Starr [e]

[a] Department of Neurosciences, University of Padova, Via Giustiniani 2, 35128 Padova, Italy
[b] Audiology and Phoniatrics Service, Treviso Regional Hospital, Piazza Ospedale 1, 31100 Treviso, Italy
[c] Servicio de Genética, Hospital Universitario Ramón y Cajal, IRYCIS, 28034 Madrid, Spain
[d] Centro de Investigación Biomédica en Red de Enfermedades Raras (CIBERER), 28034 Madrid, Spain
[e] Department of Neurology, University of California, Irvine, CA 92697, USA

ARTICLE INFO

Article history:
Received 17 December 2014
Received in revised form
21 June 2015
Accepted 12 July 2015
Available online 15 July 2015

Keywords:
Auditory neuropathy
Electrocochleography
Cochlear implant
Hearing aids
Ribbon synaptic disorders

ABSTRACT

Mutations in the *OTOF* gene encoding otoferlin result in a disrupted function of the ribbon synapses with impairment of the multivesicular glutamate release. Most affected subjects present with congenital hearing loss and abnormal auditory brainstem potentials associated with preserved cochlear hair cell activities (otoacoustic emissions, cochlear microphonics [CMs]). Transtympanic electrocochleography (ECochG) has recently been proposed for defining the details of potentials arising in both the cochlea and auditory nerve in this disorder, and with a view to shedding light on the pathophysiological mechanisms underlying auditory dysfunction.

We review the audiological and electrophysiological findings in children with congenital profound deafness carrying two mutant alleles of the *OTOF* gene. We show that cochlear microphonic (CM) amplitude and summating potential (SP) amplitude and latency are normal, consistently with a preserved outer and inner hair cell function. In the majority of *OTOF* children, the SP component is followed by a markedly prolonged low-amplitude negative potential replacing the compound action potential (CAP) recorded in normally-hearing children. This potential is identified at intensities as low as 90 dB below the behavioral threshold. In some ears, a synchronized CAP is superimposed on the prolonged responses at high intensity. Stimulation at high rates reduces the amplitude and duration of the prolonged potentials, consistently with their neural generation. In some children, however, the ECochG response only consists of the SP, with no prolonged potential. Cochlear implants restore hearing sensitivity, speech perception and neural CAP by electrically stimulating the auditory nerve fibers.

These findings indicate that an impaired multivesicular glutamate release in *OTOF*-related disorders leads to abnormal auditory nerve fiber activation and a consequent impairment of spike generation. The magnitude of these effects seems to vary, ranging from no auditory nerve fiber activation to an abnormal generation of EPSPs that occasionally trigger a synchronized electrical activity, resulting in high-threshold CAPs.

1. Introduction

Auditory neuropathy (AN) is a hearing disorder characterized by a disrupted temporal coding of acoustic signals in the auditory nerve fibers resulting in impairment of auditory perceptions relying on temporal cues. Speech perception, gap detection and the spatial localization of sounds are affected as a consequence. The magnitude of these perceptual changes is independent of the changes in audibility (Starr et al., 1996, 1998, 2008; Zeng et al., 2005).

The mechanisms believed to be involved are functional alterations at pre- and post-synaptic sites, including inner hair cell (IHC) depolarization, neurotransmitter release from ribbon synapses, spike initiation in auditory nerve terminals, loss of nerve fibers and

* Corresponding author. Department of Neurosciences, Audiology and Phoniatrics Service, University of Padova, Via Giustiniani 2, I-35128 Padova, Italy.
E-mail address: rosamaria.santarelli@unipd.it (R. Santarelli).

http://dx.doi.org/10.1016/j.heares.2015.07.007
0378-5955/

the neural dys-synchrony accompanying demyelination (Starr et al., 2003, 2004). Physiological measures of outer hair cell (OHC) activity, such as otoacoustic emissions (OAEs) and cochlear microphonics (CMs), are typically normal (Berlin et al., 2010; Starr et al., 1996, 2001). A dys-synchronous auditory nerve activity is apparent from an attenuated amplitude and a delay in auditory brainstem responses (ABRs) (Starr et al., 1996, 2008).

A frequent cause of presynaptic AN is associated with mutations of the *OTOF* gene (DFNB9) (Rodríguez-Ballesteros et al., 2003; Varga et al., 2003), which encodes otoferlin, a transmembrane protein belonging to the ferlin protein family and involved in glutamate neurotransmitter release at the ribbon synapse of IHCs. The abnormalities of neurotransmitter release are accompanied by impaired auditory nerve fiber activation. This would result in both dys-synchrony of auditory nerve activity and a decreased input to the auditory brainstem pathways, leading in turn to variable amounts of hearing loss and impaired temporal processing of acoustic information.

In this paper, we first review the spectrum of deafness-causing mutations in the *OTOF* gene and the proposed pathophysiological mechanisms underlying the impairment of auditory nerve activation, then we focus on the relationship between the audiological phenotype and the auditory nerve activity recorded using transtympanic electrocochleography (ECochG). The latter provides quantitative measures of changes in both IHC receptor potentials and auditory nerve terminal activities in response to acoustic stimuli.

2. Spectrum of *OTOF* mutations

Otoferlin is encoded by the *OTOF* gene, which lies in the chromosomal region 2p23.1. It spans 101,495 bp and contains 49 exons (named 1 to 48, plus 5′UTRsf1, an alternative exon located between exons 19 and 20). The use of different transcription and translation start sites, together with alternative exon 6, 31 and 47 splicing, generate diverse mRNAs that encode a variety of isoforms of otoferlin. All isoforms are anchored to the membrane through a transmembrane segment located near the C-terminus of the protein. Otoferlin isoforms specific to the inner ear have a transmembrane segment encoded by exon 48, whereas this segment is encoded by exon 47 in brain-specific isoforms (Yasunaga et al., 2000).

Otoferlin is a member of the ferlin family of cytosolic proteins, which contain several repeats of a structural module called the C2 domain (Yasunaga et al., 1999). Many (but not all) C2 domains can bind calcium and phospholipids. Long isoforms of otoferlin have six C2 domains (named C2A to C2F), while the short isoforms contain only three (named C2D to C2F) (Yasunaga et al., 2000). It has been demonstrated experimentally that C2A is the only C2 domain of otoferlin unable to bind calcium (Johnson and Chapman, 2010; Ramakrishnan et al., 2009; Roux et al., 2006).

Studies performed in mice indicate that, in the mature cochlea, otoferlin is located almost exclusively in the IHCs, most of the protein in their basolateral part, apparently in association with the synaptic vesicles surrounding the ribbon, or close to the presynaptic plasma membrane (Roux et al., 2006). Otoferlin might have a dual role in synaptic vesicle exocytosis, as a calcium sensor for synaptic vesicle fusion (Roux et al., 2006), and as a priming factor enabling fast vesicle replenishment (Pangršič et al., 2010, 2012).

The currently-known spectrum of sequence variants of the *OTOF* gene includes more than 90 pathogenic mutations and over 50 neutral variants (Mahdieh et al., 2012; Rodríguez-Ballesteros et al., 2008). Pathogenic variants are responsible for the DFNB9 type of autosomal recessive non-syndromic hearing impairment (Yasunaga et al., 1999).

Mutations in *OTOF* account for 1.4–5% of cases of autosomal recessive non-syndromic hearing impairment in the populations that have been studied to date (Choi et al., 2009; Duman et al., 2011; Hutchin et al., 2005; Iwasa et al., 2013; Jin et al., 2014; Mahdieh et al., 2012; Rodríguez-Ballesteros et al., 2003; Romanos et al., 2009; Varga et al., 2006). These mutations have been found in very different proportions in cohorts of subjects from several countries, ranging from about 5% in some Chinese and Korean studies, through 50–60% in studies from the USA, Brazil and Japan, to 86% in Spanish cohorts (Bae et al., 2013; Chiu et al., 2010; Jin et al., 2014; Matsunaga et al., 2012; Rodríguez-Ballesteros et al., 2008; Romanos et al., 2009; Varga et al., 2006; Wang et al., 2010). This wide range of frequencies may reflect an actual diversity between populations, as exemplified by the very high frequency seen in the Spanish population, which is probably related to a genetic founder effect for a single, very frequent mutation. It should be noted, however, that the sizes of the cohorts studied were small and the criteria adopted for including subjects in the various cohorts were not homogeneous, and this could strongly bias the results.

Most patients present with a very homogeneous phenotype of severe-to-profound congenital hearing loss. Over 50% of children carrying two mutant alleles of the *OTOF* gene have a preserved OHC function as indicated by CM and OAE recordings (Rodríguez-Ballesteros et al., 2003; Varga et al., 2003). The disappearance of OAEs over time has been reported in some patients with otoferlin-related mutations as possibly reflecting delayed damage to OHCs (Rodríguez-Ballesteros et al., 2003; Chiu et al., 2010).

About 75% of *OTOF* pathogenic mutations are clearly inactivating (sometimes named truncating). This group includes large deletions that remove numerous exons, nonsense mutations, small duplications and deletions that lead to frameshifts giving rise to premature stop codons, and splice-site mutations that result in exon skipping. These mutations could lead to the synthesis of truncated polypeptides, but it is very likely that their mRNAs are degraded by nonsense-mediated decay and thus, no polypeptide would be synthesized. All these mutations are associated with a phenotype of severe-to-profound prelingual hearing impairment (Rodríguez-Ballesteros et al., 2008).

The remaining mutations (usually called non-truncating) are believed to result in complete polypeptides. Most of them are missense mutations, believed to result in amino acid substitutions, and there are also a few in-frame deletions that remove single amino acid residues. Remarkably, most of these changes occur within the functional domains of otoferlin (the C2 domains B to F, or the transmembrane domain; non-pathogenic variants occur mainly outside these domains). Many of these mutations are also associated with a phenotype of severe-to-profound prelingual hearing impairment, suggesting that the proteins are not functional, probably due to enhanced degradation (Rodríguez-Ballesteros et al., 2008). Some mutations of this group deviate from the usual phenotype, however, suggesting a conditional or residual function of the mutated proteins. Among them, six mutations (p.I515T, p.G541S, p.G614E, p.R1080P, p.R1607W, and p.E1804del) have been reported in patients with a temperature-sensitive phenotype (Marlin et al., 2010; Matsunaga et al., 2012; Romanos et al., 2009; Varga et al., 2006; Wang et al., 2010). In addition, mutation p.E1700Q (which affects a residue in the linker region between domains C2E and C2F) results in progressive hearing loss that may range in severity from mild to profound (Chiu et al., 2010). One child carrying this mutation, who had no ABRs but did have OAEs at six months of age, showed progressive worsening of hearing thresholds and disappearance of OAEs by the age of 3 years.

3. *OTOF* gene mutations result in pre-synaptic auditory neuropathy

In the healthy cochlea, the dynamics of receptor potentials and auditory nerve fiber activation are well suited to fast and precise signal transmission (Moser et al., 2006). At presynaptic level, the temporal precision of acoustic signaling is guaranteed by the rapid kinetics of synaptic release, triggered by calcium influx through one or two calcium channels, tight coupling of these channels to the vesicle release sites, and a parallel release of multiple vesicles through the ribbon synapses. These specialized synapses contain an electron-dense body, the ribbon, that enables the rapid release of hundreds of glutamate-containing vesicles in response to graded receptor potentials (Buran et al., 2010). High glutamate release rates lead to the generation of excitatory post-synaptic potentials (EPSPs), which trigger spike initiation in the auditory nerve fibers through AMPA receptor activation (Glowatzki and Fuchs, 2002). These receptors have a low affinity for glutamate, and this results in quick post-synaptic membrane activation and de-activation times, thus ensuring that nerve fiber sensitivity is preserved despite the large amounts of neurotransmitter being released in the synaptic cleft. At auditory nerve level, the velocity and precision of spike initiation and propagation are guaranteed by the abundance of Nav1.6 channels and their strategic distribution along the nerve fibers (Hossain et al., 2005).

The disruption of any one of these mechanisms interferes with the precise temporal coding of acoustic signals. At presynaptic level, an impaired multivesicular release results in a more limited neurotransmitter availability at the synaptic cleft, with the generation of small EPSPs that have an abnormal morphology and are dispersed in time (pre-synaptic AN) (Santarelli et al., 2009; Starr et al., 2008; Wynne et al., 2013). At post-synaptic level, decreasing numbers of auditory nerve fibers and demyelination of the spared axons result in a lower auditory input to the central nervous system and a slower conduction velocity in the residual fibers (post-synaptic AN) (Starr et al., 2003, 2008; Wynne et al., 2013).

The most well-known forms of AN are due to gene mutations and may present as isolated hearing disorders or associated with multisystem involvement (Santarelli, 2010; Starr et al., 2000, 2008). In general, most isolated forms of AN are associated with presynaptic mechanisms, whereas AN disorders with multisystem involvement are typically due to post-synaptic mechanisms that affect both auditory and peripheral nerves.

One well-studied form of presynaptic AN is caused by mutations in the *OTOF* gene (Rodríguez-Ballesteros et al., 2003, 2008; Santarelli et al., 2009; Starr et al., 1998; Varga et al., 2003). Otoferlin has been implicated in multivesicular release at the synapse between the IHCs and auditory nerve fibers. The rapid phase of exocytosis is abolished in IHCs of knock-out mice (Roux et al., 2006) and this condition is not reversed by fast Ca++ influx or Ca++ uncaging (Pangršič et al., 2012). These findings support the hypothesis that otoferlin acts as a Ca++-sensor that triggers vesicle fusion with the presynaptic membrane (Roux et al., 2006). In this view, the absence of otoferlin or its alteration can be expected to interfere with the precise timing of acoustic signals, particularly at high frequencies, with a consequent dys-synchrony of auditory nerve fiber activation and spiking.

Another function for otoferlin has been proposed in the light of the effects of the missense mutation in the C2–F domain in the pachanga mouse, which results in a slower replenishment of the readily-releasable pool of vesicles at the synaptic pole of IHCs (Pangršič et al., 2010). The availability of a large, rapidly-releasable pool of synaptic vesicles is designed to ensure a fast and precise acoustic coding through the release of large amounts of neurotransmitter within a very short time. This priming function is expected to be closely connected to the synchronization of auditory nerve fiber discharge. Slowing the stimulation rate in the profoundly deaf pachanga mouse results in better neural spiking in single auditory nerve fibers at sound onset, consistent with the hypothesis that the fast phase of exocytosis also relies on the availability of a promptly-releasable pool of vesicles.

Otoferlin has recently been found to interact with AP-2 and myosin VI, two proteins involved in clathrin-mediated endocytosis (Duncker et al., 2013), which is essential to synaptic vesicle replenishment. On these grounds a further role for otoferlin has been suggested: it could be involved in coupling exocytosis and endocytosis in IHCs, thus providing the basis for sustained release at the ribbon synapse.

4. Clinical features of *OTOF*-Related auditory neuropathy

Most patients carrying two mutant alleles of the *OTOF* gene have congenital severe-to-profound hearing loss and absent ABRs (Rodríguez-Ballesteros et al., 2003, 2008; Santarelli et al., 2009; Varga et al., 2003, 2006). Lesser degrees of hearing loss have been reported in subjects carrying some missense *OTOF* mutations. Otoferlin may retain a residual function in such cases, with hearing preserved to some degree (Chiu et al., 2010; Matsunaga et al., 2012). Unfortunately, speech perception was not assessed systematically in these patients.

Some individuals harboring missense mutations in the *OTOF* gene suffer from a particular disorder called temperature-sensitive auditory neuropathy (Marlin et al., 2010; Starr et al., 1998; Varga et al., 2006; Wynne et al., 2013). When afebrile, these patients have normal or only mildly elevated hearing thresholds. When their core temperature rises, their hearing thresholds increase, leading to variable degrees of hearing loss. Profound deafness has been documented in some patients with a temperature increase of 1 °C. Speech perception has been assessed in these patients in both quiet and noisy conditions, using several tests such as the PBK-word and the hint sentence recognition tests, and speech reception threshold measures (Starr et al., 1998; Marlin et al., 2010; Varga et al., 2006). In afebrile conditions, speech perception is normal or only slightly impaired in quiet environments, but it is abnormally reduced in the presence of background noise (Starr et al., 1998; Varga et al., 2006). Speech perception deteriorates when the core temperature rises, invariably becoming impaired even in quiet environments regardless of the extent of the individual's hearing threshold elevation (Starr et al., 1998; Marlin et al., 2010; Matsunaga et al., 2012; Varga et al., 2006).

Wynne et al. (2013) recently studied adaptation in patients with temperature-sensitive AN by measuring the perceived loudness changes during the presentation of a continuous tone with a fixed intensity for 3 min. The results were compared with findings collected respectively in a group of normally-hearing subjects and a group of patients with post-synaptic forms of AN (Fig. 1, left panel). No change in loudness was perceived by the normally-hearing controls during tone stimulation. In contrast, an abnormal loudness adaptation occurred in the subjects with temperature-sensitive AN, even when they were afebrile, and the change in loudness was significantly greater in response to stimulation with high-as opposed to low frequency tones. Adaptation was more rapid and of greater magnitude in temperature-sensitive AN than in post-synaptic forms of auditory neuropathy, with the latter only showing an abnormal adaptation to high-frequency tones.

Loudness adaptation during steady stimulation was paralleled by changes in Wave V amplitude and latency evoked by rapid trains of clicks. Fig. 1 (right panel) shows averaged ABR recordings obtained in response to each click in a train sequence (20 clicks, inter-

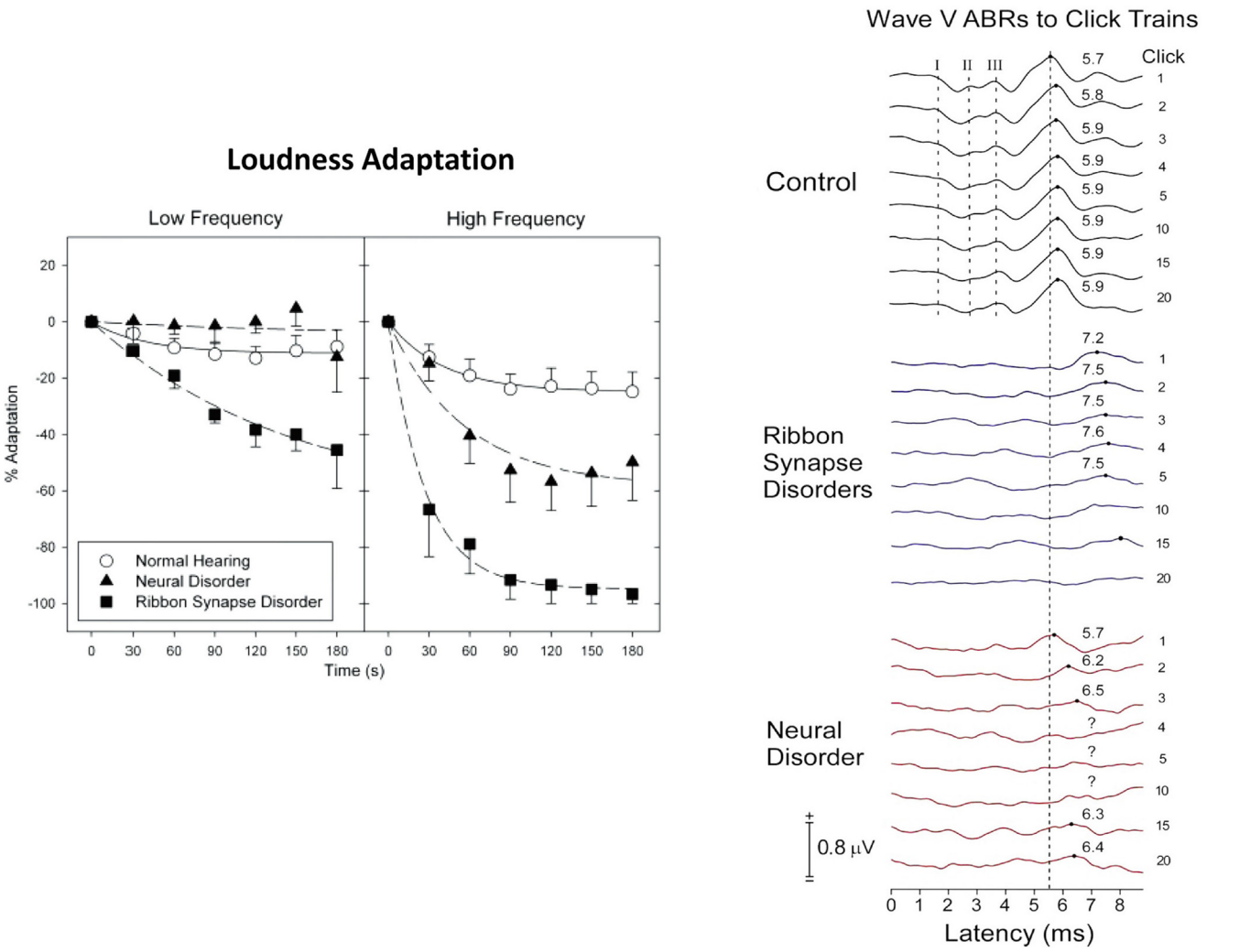

Fig. 1. Adaptation in subjects with temperature-sensitive AN. Loudness adaptation (left panel) at low and high frequencies for subjects with ribbon synapse disorder (filled squares) is compared with normally-hearing individuals (open circles) and patients with post-synaptic AN (filled triangles). Patients with ribbon synapse disorders showed an abnormal loudness adaptation, and the magnitude of this effect was more pronounced at high frequency. An abnormal adaption was only seen in subjects with post-synaptic AN at high frequency, and it was significantly lower than in patients with temperature-sensitive AN. Averaged ABR recordings (right panel) obtained in response to each click in a train sequence (20 clicks, inter-click interval 13 ms, inter-train interval 553 ms) are shown on the right for normally-hearing individuals, patients with temperature-sensitive AN, and subjects with auditory nerve disorders. A different wave V adaptation pattern emerged between cases of ribbon synapse and neural disorders. (Modified with permission from Wynne et al., Brain 2013; 136: 1626–1638).

click interval 13 ms, inter-train interval 553 ms) from normally-hearing individuals, subjects with temperature-sensitive AN tested when afebrile, and patients with a hereditary neuropathy affecting the auditory nerve. In the normally-hearing subjects, Wave V was identified in response to every click in the train. Wave V latency was 5.7 ms in response to the first click, and increased to 5.9 ms by the third click in the train, whereas Wave V amplitude remained relatively constant throughout the click sequence. In the patients with temperature-sensitive AN, Wave V was of low amplitude and delayed latency (7.2 ms) in response to the first click of the train, with a further delay in latency (7.5 ms) in response to the next 4 clicks, and was then absent in response to subsequent clicks. These findings suggest that neurotransmitter release is reduced at the onset of acoustic stimuli in temperature-sensitive AN, and becomes further impaired during sustained stimulation. In subjects showing post-synaptic AN, the initial click of the train evoked a Wave V of normal latency (5.7 ms) whereas Wave V was absent or delayed in response to subsequent clicks, consistently with an auditory nerve fiber conduction block. On the basis of these findings, the authors concluded that differences in loudness adaptation between temperature-sensitive ribbon synapse disorders and post-synaptic neural AN likely reflect the failure of sustained neurotransmitter release with sustained stimulation in the former, and neural conduction changes in the latter.

The majority of subjects carrying mutations in the *OTOF* gene present with a very homogeneous phenotype of congenital profound hearing loss. Eight hearing-impaired children with mutations involving the two alleles of the *OTOF* gene have been diagnosed and followed up at the University of Padua Service of Audiology and Phoniatrics in the last ten years, while their genetic analyses were performed at the Hospital Ramón y Cajal in Madrid. Details of their genetic findings together with clinical and audiological results are summarized in Table 1, while the location of their pathogenic mutations in the *OTOF* gene is shown in Fig. 2. Four subjects had truncating mutations in both alleles, three children, who were siblings, had a truncating mutation in one allele and a non-truncating mutation in the other, and the remaining child had a non-truncating mutation in both alleles.

Table 1
Clinical and Audiological data from *OTOF* patients.

Subjects#	#1	#2	#3	#4	#5	#6	#7	#8
Clinical								
Gender	M	F	F	M	M	M	M	M
Age tested	1 year	1 year	2 years	2 years	1 year	1 year	4 months	2 years
Genotype	p.Arg1134*/ p.Trp1739*	p.Val537*/ p.Arg656Glyfs*10	p.Glu747*/ pGlu747*	p.Pro534Glnfs*4/ p.Tyr913Alafs*90	p.Tyr913Alafs*90/ p.Ala964Glu	p.Tyr913Alafs*90/ p.Ala964Glu	p.Tyr913Alafs*90/ p.Ala964Glu	p.Phe1795Cys/ p.Phe1795Cys
Mutation Classification	Truncating/ Truncating	Truncating/ Truncating	Truncating/ Truncating	Truncating/ Truncating	Truncating/ Non-truncating	Truncating/ Non-truncating	Truncating/ Non-truncating	Non-truncating/ Non-truncating
Audiology	R/L							
Deafness	Profound	Profound	Profound	Profound	Profound	Profound	Profound	Profound
PTA (dB HL)	121	120	107	114	120	109	113	114
OAEs	+/+	+/+	+/+	+/+	+/+	+/+	+/+	+/+
ABRs	−/−	−/−	−/−	−/−	−/−	−/−	−/−	−/−
ECochG	R/L							
Pattern	A/A	B/A	A/B	C/C	C/C	A/A	A/A	B/B
Prolong THR (dB SPL)	60/90	60/80	70/60	–	–	50/60	60/60	70/70
Prolong THR (dB nHL)	30/60	30/50	40/30	–	–	20/30	30/30	40/40
Cochlear Implant								
CI	yes	CI24RE	CI24RE	CI24RE	CI24RE	CI24RE	CI512	yes
Ear	–	Right	Left	Right	Right	Right	Right	–
HA	yes	yes	yes	yes	yes	yes	yes	yes
Age at implant (yrs)	–	4	2	2	2	1.5	1	–
Disyllable Recognition	–	95%	95%	100%	90%	100%	95%	–

R/L = right ear/left ear; PTA = pure tone average (average thresholds at 0.5, 1, 2, 4 kHz); OAEs = otoacoustic emissions; ABRs = auditory brainstem responses; Prolong THR = threshold of the prolonged potential; CI = cochlear implant; HA = hearing aid.

All the children underwent ABR and OAE recording, and completed a behavioral audiometry. They were all tested with transtympanic electrocochleography (ECochG) as part of the objective measurement of their cochlear and auditory nerve function before undergoing cochlear implantation.

An example of the audiological findings collected from one child (Subj. #2) is shown in Fig. 3. Visual reinforcement audiometry performed in the free field indicated a profound hearing loss with some residual hearing at low frequencies. ABR recordings showed no evoked responses, while distortion product otoacoustic emissions (DPOAEs) were detected bilaterally. The use of power hearing aids resulted in a considerable improvement in pure tone sensitivity (Santarelli et al., 2013a).

Similar results were obtained in all the other children carrying *OTOF* mutations. They were all fitted with power hearing aids before undergoing cochlear implantation. Fig. 4 shows the means and standard errors for the unaided and aided hearing thresholds obtained for all the children using visual reinforcement

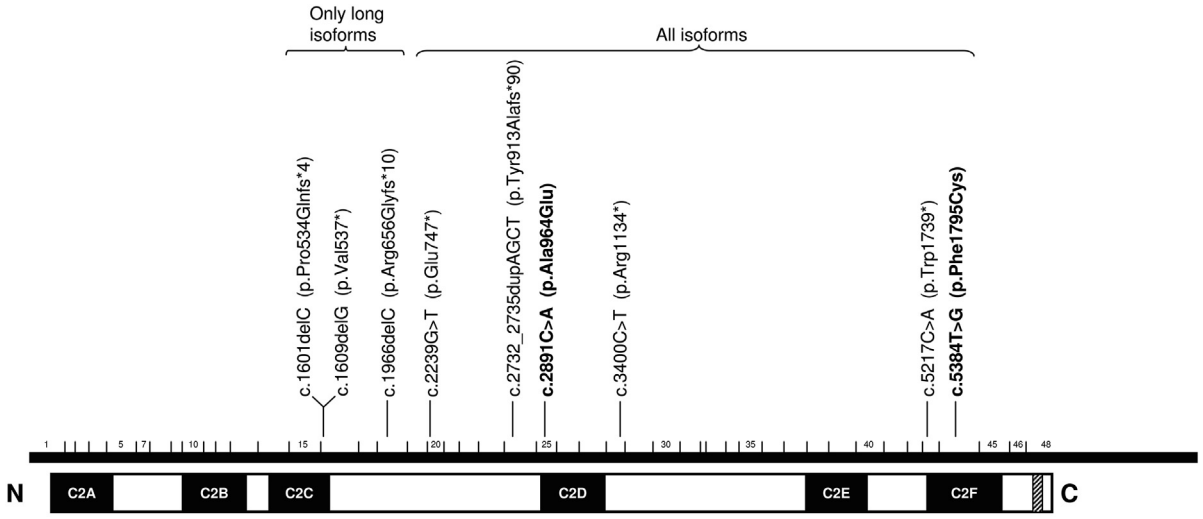

Fig. 2. Location of the pathogenic mutations in the *OTOF* gene found in the patients reviewed in this study. Vertical lines indicate the position of each mutation on the reference cDNA (accession number AF183185.1) and on the correlated position in the protein. A horizontal bar depicts the cDNA, and small vertical bars delimit the exons, which are numbered. The reference cDNA does not contain exon 6. Exon 47 has been removed from the figure, as it is not present in the cochlear isoforms of the protein. Black boxes represent the C2 domains, whereas the cross-hatched box represents the transmembrane domain. Missense mutations are shown in bold. Curly brackets on the top of the figure indicate which mutations affect only the long isoforms of otoferlin, and which affect all isoforms.

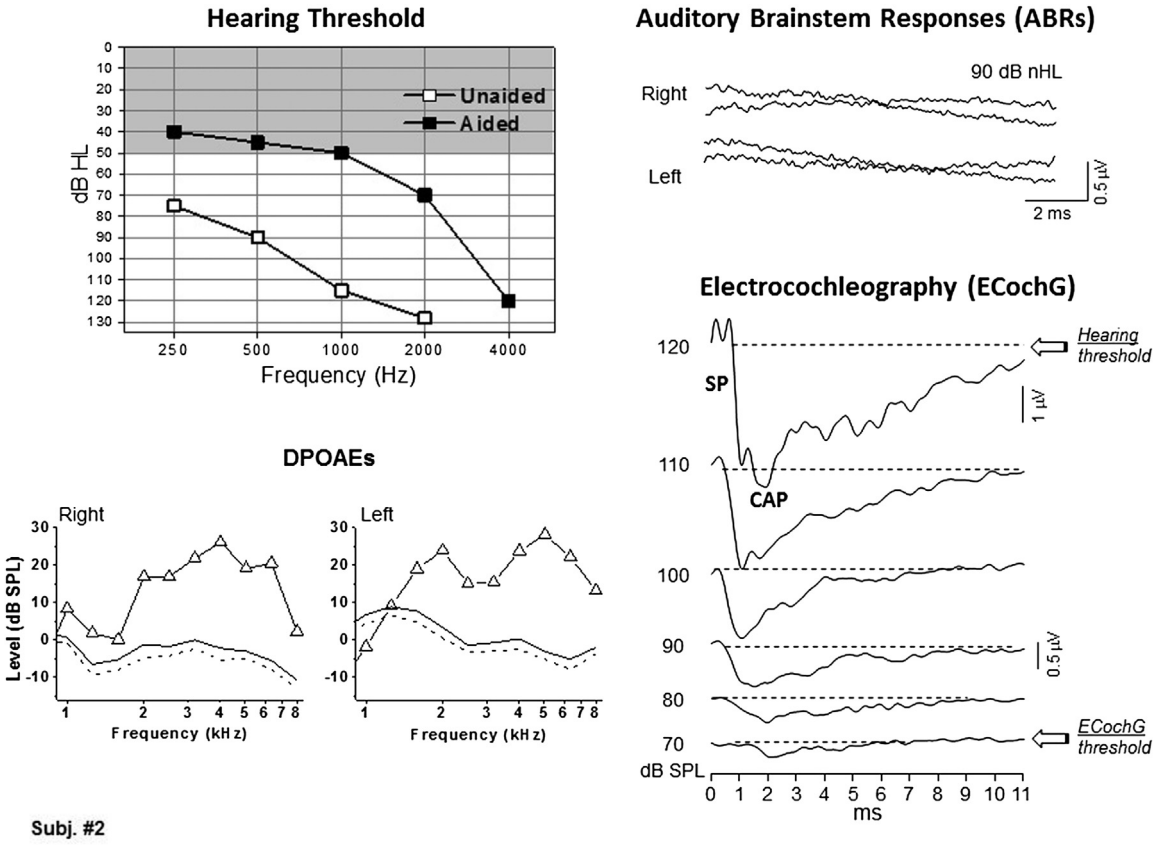

Fig. 3. Hearing thresholds and DPOAEs, ABRs and ECochG recordings collected from one child carrying two mutant alleles of the *OTOF* gene (subject #2). The audiometric assessment performed in the free field using visual reinforcement audiometry is shown in the upper left panel. Both unaided and aided thresholds are shown, the latter obtained with the child wearing both hearing aids. Note that the functional gain was good, but the aided thresholds were beyond the intensity range calculated for conversational speech (shadowed rectangle). DPOAEs were detected in both ears (lower left), whereas ABRs were absent (upper right). ECochG recordings (lower right) showed the summating potential (SP) followed by a prolonged negative response, recorded as low as 70 dB SPL (corresponding to 40 dB nHL) despite the profound hearing loss identified at audiometry. The compound action potential (CAP) was superimposed on the prolonged response at high intensity. In this and subsequent figures, the time "0" refers to CM onset, the horizontal lines indicate the baseline. (Modified with permission from Santarelli et al., Semin Hear 2013; 34: 51–64).

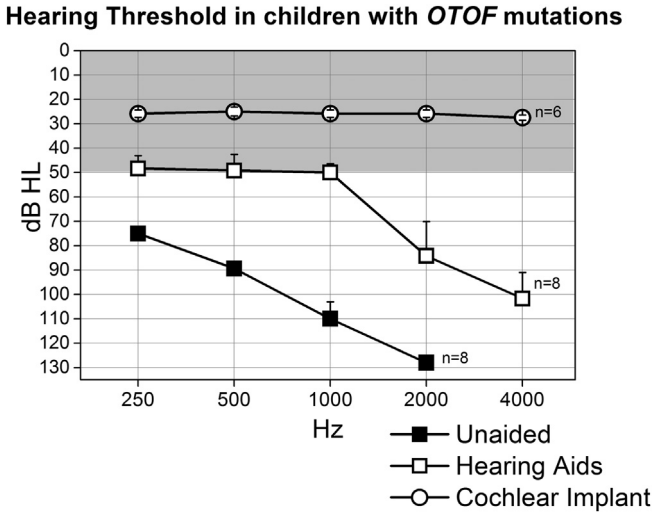

Fig. 4. Means and standard errors of unaided (closed squares) and aided (open symbols) hearing thresholds in children with *OTOF* gene mutations. Mean aided thresholds, obtained with children wearing both hearing aids (open squares), indicated improvements in hearing sensitivity, but they fell beyond the intensity range of conversational speech (shadowed rectangle). In contrast, hearing thresholds obtained using the cochlear implant (open circles) showed a restored hearing sensitivity from the low to the high frequencies.

audiometry. Profound deafness was identified, with some residual hearing at frequencies below 1 kHz. Aided thresholds (measured with the children wearing both hearing aids) showed a marked improvement in pure tone sensitivity, particularly at the frequencies showing some residual hearing; however, they proved to be above the intensity range of conversational speech (Boothroyd, 2008). These findings suggest that increasing the sound level by means of acoustic amplification is likely to result in a greater glutamate release at the ribbon synapses and an enhanced auditory nerve fiber activation, with a consequent improvement in hearing sensitivity.

It was difficult to test speech perception with the hearing aids in these children due to their young age. One child (subject #2) was able to perform word identification (Speech Perception Categories by Geers and Moog, 1991), while two (subjects #4, #7) detected speech sounds (Six Sound Test).

All *OTOF* children received a cochlear implant (Table 1). The use of hearing aids might have positively influenced the outcome after cochlear implantation in terms of speech intelligibility (Artières et al., 2009) by acting as "*a bridge to auditory access to language*" (Nicholas and Geers, 2007).

5. Cochlear potentials

In recent years, the diagnostic use of ECochG recordings has been proposed for defining the details of potentials arising in the

cochlea and auditory nerve in the various forms of AN (McMahon et al., 2008; Santarelli and Arslan, 2002, 2013, 2015; Santarelli et al., 2008, 2009, 2013a, 2013b). Such information may prove extremely valuable in objectively ascertaining the site of auditory nerve dysfunction and shedding light on the underlying pathophysiological mechanisms in order to plan an appropriate rehabilitation strategy.

Bilateral ECochG recordings are part of our audiological assessment when the reliability of ABRs for estimating hearing thresholds may be reduced (Santarelli and Arslan, 2013, 2015). ECochG recordings are also part of our standard assessment protocol in candidates for cochlear implants. We record ECochG potentials through a transtympanic approach by using a sterile stainless steel needle electrode placed on the promontory wall. In children, ECochG recordings are performed under general anesthesia. The stimuli, usually clicks, are presented in the free field with a maximum intensity of 120 dB p.e. (peak equivalent) SPL (corresponding to 90 dB nHL when referred to the psychoacoustic threshold of normally-hearing individuals).

ECochG responses result from the superimposition of three components, two originating from receptor elements, the cochlear microphonic (CM) and the summating potential (SP), and the third, the compound action potential (CAP), arising from the synchronous activation of auditory nerve fibers innervating the basal portion of the cochlea (Eggermont, 1976). CM responses are believed to originate mainly from the sum of the extracellular components of receptor potentials arising from OHCs located in the basal cochlear region (Dallos and Cheatham, 1976). SP responses recorded from the promontory wall originate from the DC component of receptor potentials arising in the basal IHCs (Durrant et al., 1998). Receptor and neural activities are intermingled in ECochG waveforms, often preventing the identification of individual components. Since CM activity is strictly related to basilar membrane motion, the procedure of averaging the potentials evoked separately by condensation and rarefaction stimuli is generally used to extract both the SP and the CAP components (Eggermont, 1976).

Fig. 5 shows ECochG waveforms recorded in response to clicks at decreasing stimulus intensities for a normally-hearing control and a child carrying two mutant alleles of the *OTOF* gene (Subj. #1). The CM potential appears as an oscillatory activity identified as low as 90 dB SPL in both the normal control and the *OTOF* patient with comparable amplitudes. In the normal control, the ECochG waveform resulting from CM cancellation at high intensity begins with an abrupt negative deflection, the SP, followed by a negative peak, the neural CAP (Eggermont, 1976; Elberling, 1976). Decreasing the stimulus level results in a gradual latency increase and amplitude reduction of both SP and CAP peaks. The duration of the SP-CAP complex, as measured from SP onset to return to baseline, is relatively constant at suprathreshold intensities (1.5–2 ms), but increases at lower stimulation levels of about 1–2 ms.

In the majority of *OTOF* children, the ECochG responses recorded at high intensity begin with a rapid negative deflection that peaks

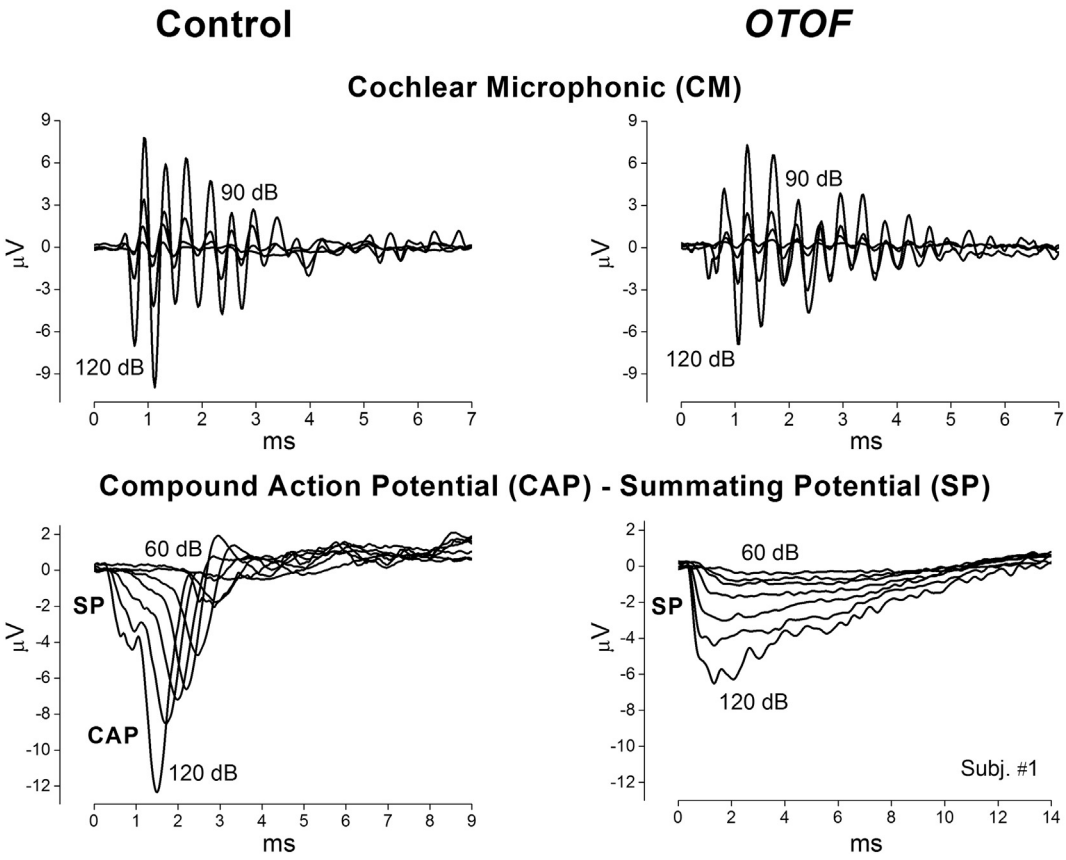

Fig. 5. Cochlear potentials recorded in a normally-hearing individual and in a child with mutations in the *OTOF* gene (Subj. #1) in response to clicks at decreasing stimulation intensities. The cochlear microphonic (CM) was recorded in the *OTOF* child with control amplitudes. After CM cancellation, the ECochG waveforms recorded from the normal control consisted of a fast negative deflection, the receptor summating potential (SP), followed by the neural compound action potential (CAP). Decreasing the stimulus level resulted in a gradual latency increase and amplitude reduction of both SP and CAP peaks. In the child with *OTOF* mutations the ECochG responses began with a fast negative deflection, peaking at the same SP peak latency as in the normal control and showing a comparable amplitude. This was followed by a low-amplitude, negative potential with markedly prolonged duration compared with the CAP recorded in the control.

at the same SP peak latency as in the normal control and is of a comparable amplitude. This is followed by a low-amplitude negative potential showing a markedly prolonged duration compared with the CAP recorded in the control, which returns to baseline at approximately 13–14 ms after the onset of the response. This prolonged potential was recorded at stimulus intensities well below the behavioral threshold in all *OTOF* patients. This is shown in the example in Fig. 3, where the prolonged negative response was identified as low as 70 dB SPL (corresponding to 40 dB nHL) despite the profound hearing loss found at audiometry. The differences between the behavioral thresholds and the threshold of the prolonged potential in all subjects are apparent from Table 1. The pure tone average (PTA) thresholds at 0.5, 1, 2 and 4 kHz, measured in the free field, appear markedly higher than the threshold of the prolonged response in each child.

Three patterns of ECochG potentials were observed in the *OTOF* children (Fig. 6, Table 1). In the most common pattern ("A" in Fig. 6), identified in eight ears, only the prolonged response was recorded, without any superimposed CAP (Fig. 6, upper panel). The second pattern ("B" in Fig. 6) was seen in four ears and consisted of a small CAP, peaking at the same CAP peak latency as in controls, which was superimposed on the prolonged negative activity at high stimulation levels (Fig. 6, middle panel; Fig. 3, lower right). In a third pattern ("C" in Fig. 6), seen in two children (subjects #4 and #5), the ECochG waveform only consisted of the initial abrupt negative component, peaking at the same SP peak latency as in controls, which was not followed by a prolonged potential. This response returned to baseline approximately 2–3 ms after the onset of the response (Fig. 6, lower panel).

The means and standard errors of the CM amplitude, and of the SP latency and amplitude are plotted in Fig. 7 as a function of signal intensity for a group of 20 normally-hearing controls (age range: 3.5–6.5 years) and for the 8 *OTOF* children. No differences in CM amplitude were found between the two groups, and this is consistent with a normal OHC activation in children carrying *OTOF* mutations. SP latencies and amplitudes were also within the control range consistent with normal IHC activation dynamics, although mean SP amplitudes appeared smaller in *OTOF* children than in normally-hearing individuals. These findings are in accordance with the results obtained by Pangršič et al. (2010), who showed normal receptor cochlear potentials (CM, SP) in the pachanga mouse model of human deafness DFNB9.

In previous papers (Santarelli and Arslan, 2002; Santarelli et al., 2008), to clarify whether the prolonged potentials recorded in various forms of auditory neuropathy originate from neural or receptor activation, we used a high-rate adaptation procedure that preferentially attenuates neural responses by taking advantage of the different effects of high stimulation rates on neural and receptor potentials (Eggermont, 1976). The stimulus sequence consisted of an initial click, followed 15 ms later by ten clicks with an inter-stimulus interval of 2.9 ms, and the sequence was repeated every 191 ms (Santarelli et al., 2008). This stimulus paradigm was also used in the *OTOF* children, except for subject #8, whose stimuli consisted of repetitive clicks presented with an inter-stimulus interval of 91 ms.

Unlike the post-synaptic forms of AN, where the synapses are believed to work normally, exocytosis, glutamate vesicle recycling and replenishment might be impaired in ribbon synaptic disorders as a consequence of otoferlin dysfunction (Pangršič et al., 2012). Thus, high stimulation rates might result in a greater attenuation of receptor SP potentials in patients carrying *OTOF* mutations than in normally-hearing controls or patients with post-synaptic AN. We therefore studied the effects of adaptation on the cochlear potentials using a low stimulus intensity to minimize the contribution of the receptor SP to the whole ECochG waveform. In fact, we reported

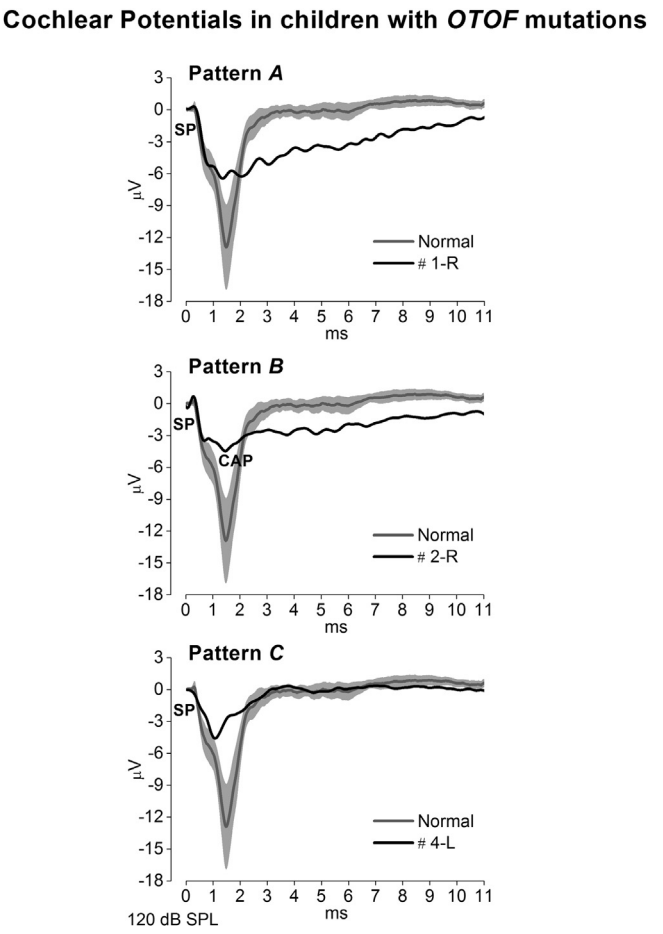

Fig. 6. Cochlear potentials recorded in children with mutations in the *OTOF* gene. Three patterns of ECochG responses were recognized at high stimulus intensity (120 dB SPL). They are superimposed on the grand average of ECochG waveforms with 95% confidence limits calculated for controls at the same intensity. In the most common pattern (pattern "A"), the summating potential (SP) was followed by a low-amplitude, negative response with markedly increased duration compared with controls. In a second pattern (pattern "B"), a small compound action potential (CAP) was superimposed on the prolonged response. In a third pattern (pattern "C"), the response only consisted of the initial fast negative component peaking at the same SP peak latency as in the normal control. R: right ear, L: left ear.

in previous papers (Santarelli and Arslan, 2013, 2015) that the SP amplitude decreases rapidly from 120 to 90 dB SPL in normally-hearing subjects. Fig. 8A shows the ECochG recordings obtained in a normally-hearing control and two children carrying *OTOF* mutations, at intensities decreasing from 100 to 70 dB SPL in response to the sequence of stimuli reported at the bottom. In the normal control, CAP amplitude at 100 dB SPL showed a marked attenuation from the first (#1) to the second (#2) click in the sequence (which corresponded to the first click in the high-rate train), then a further drop was apparent during the sustained train sequence, whereas SP amplitude showed no attenuation from the first to the last click in the sequence. A similar behavior was observed at lower intensities, but the SP component was only identified in response to the sustained train stimulation at 90 dB SPL. The duration of the ECochG waveforms, measured from SP onset to return to baseline, showed no change from the first to the last click of the stimulus sequence at each intensity.

Two patterns of adaptation were seen in the children with *OTOF* mutations. In the most common pattern (Fig. 8A, subject #6), the ECochG waveform recorded at 100 dB SPL in response to the first click of the sequence began with a rapid negative deflection that

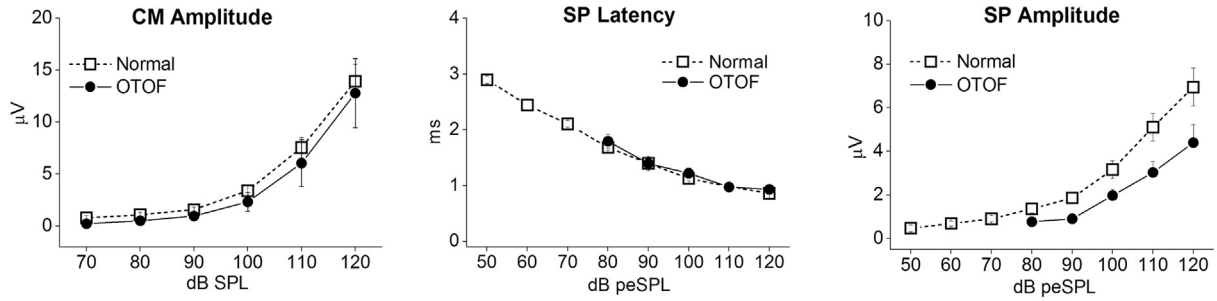

Fig. 7. Means and standard errors of CM amplitudes and SP peak latencies and amplitudes at increasing stimulation intensities are shown for *OTOF* children (closed circles) and normally-hearing controls (open squares). No significant differences in CM amplitudes or SP latencies and amplitudes were found between the two groups.

peaked at the same SP peak latency as in the normal control, and was followed by the prolonged negative potential. The early, rapid SP component was also identified in response to the following high-rate clicks. At intensities below 100 dB, the ECochG waveform failed to show the initial rapid component, and only consisted of the prolonged negative potential peaking at the same latency as the CAP in the normal control. The duration of this potential decreased during adaptation, and dropped to control values by the last click in the sequence, while response amplitude was markedly attenuated. This pattern of decreasing amplitude and duration after adaptation was seen in 4 of the 7 *OTOF* children tested (subjects #1, #2, #3, #6).

A different adaptation pattern was seen in the two children (subjects #4, #5) showing no prolonged ECochG potentials. In the example in Fig. 8A (subject #4), a rapid stimulation rate induced no

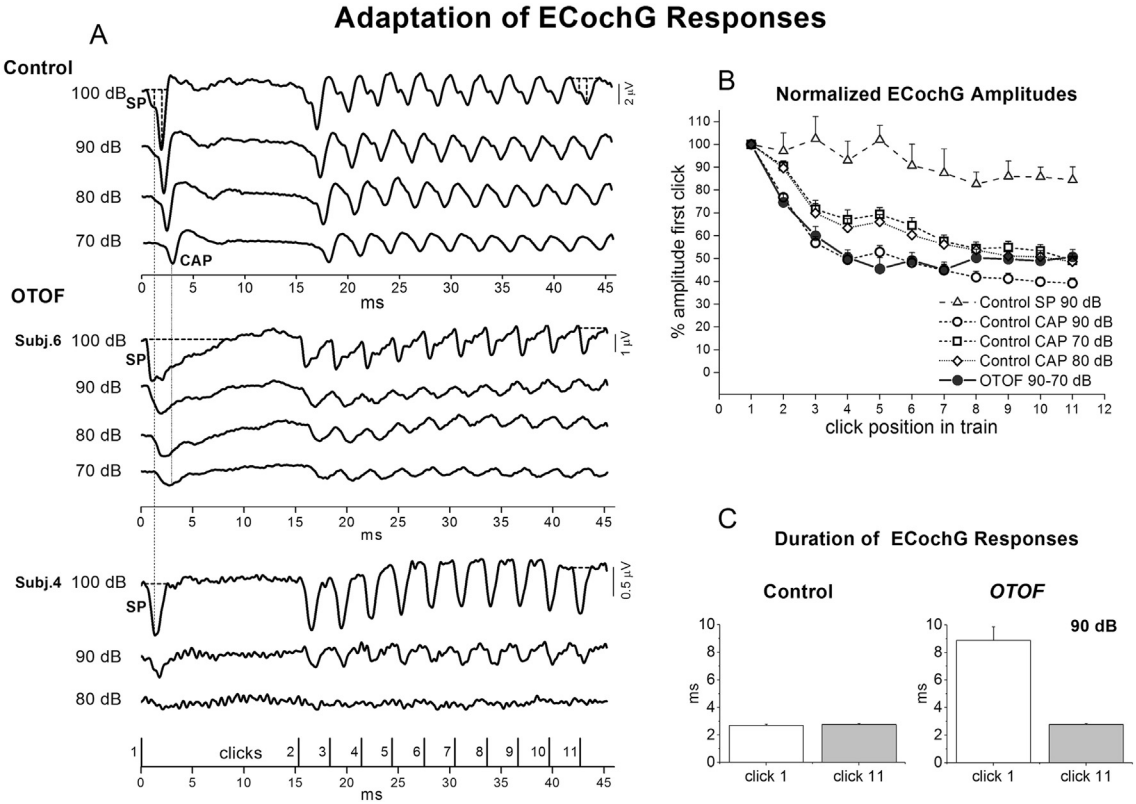

Fig. 8. Adaptation of ECochG potentials in *OTOF* patients. The left panel (A) shows the ECochG recordings obtained at intensities from 100 to 70 dB SPL from one normally-hearing control and two *OTOF* children in response to the stimulus sequence shown at the bottom. In the normal control (upper trace), CAP amplitude (as measured from the baseline to the CAP peak) was markedly attenuated after adaptation, whereas SP attenuation was much smaller. In the adaptation pattern seen in *OTOF* subject #6 (middle trace) the ECochG waveforms were markedly attenuated after adaptation and the duration of the response decreased to control values from the first to the last click in the sequence. In the adaptation pattern observed in subject #4 (lower trace) there was no evidence of any response attenuation or change in duration at high stimulation rates. The vertical dashed lines refer respectively to the SP peak at 100 dB and the CAP peak at 70 dB in the normal control. The right upper panel (B) shows the means and standard errors of normalized amplitudes of ECochG potentials as a function of click position in the stimulus sequence, for the group of normally-hearing controls and the four *OTOF* patients showing adaption of the ECochG responses. For the normally-hearing controls, mean CAP amplitudes are shown separately for intensities from 90 to 70 dB SPL together with the mean SP amplitudes obtained at 90 dB SPL. For the *OTOF* children, the mean amplitudes of the ECochG potentials were obtained by averaging individual response amplitudes at intensities from 90 to 70 dB SPL. In children with *OTOF* mutations the degree of cochlear potential attenuation during adaptation was within the range of CAP attenuation calculated for controls at intensities from 90 to 70 dB SPL. The right lower panel (C) shows the means and standard errors of the ECochG waveform durations calculated for the first (#1) and last click (#11) of the stimulus sequence, for both normally-hearing controls and *OTOF* children, at an intensity of 90 dB SPL (same sample as in B). The duration of the normal controls' cochlear potentials did not change at high stimulus rates, whereas in *OTOF* children the duration of the ECochG waveforms decreased to control values during adaptation.

change in either amplitude or duration after adaptation.

Unlike all the other *OTOF* patients, subject #7 showed no response to the sustained train sequence (from the second to the eleventh click) at intensities below 110 dB SPL.

In Fig. 8B the means and standard errors of ECochG response amplitudes calculated for the group of normally-hearing controls and the four *OTOF* children showing adaptation of the prolonged responses (subjects #1, #2, #3, #6) are reported as a function of click position in the stimulus sequence at intensities from 90 to 70 dB SPL. In the normally-hearing controls, CAP and SP peak amplitudes were measured relative to the baseline of 1 ms immediately preceding CM onset. In *OTOF* patients, the amplitude of the ECochG waveform was measured from the baseline to the peak of the prolonged response. In both normally-hearing controls and *OTOF* children amplitudes were normalized to the first click in the sequence.

In normally-hearing controls, the mean CAP amplitude obtained at 90 dB SPL dropped by 23% from the first to the second click, and showed an additional attenuation in the subsequent stimuli, reaching a reduction of 61% by the end of the stimulus sequence. The mean CAP attenuation at 80 and 70 dB SPL was 10–15% smaller than the reduction calculated at 90 dB SPL (Santarelli and Arslan, 2013). The attenuation in SP amplitude after adaptation could only be measured reliably at 90 dB SPL in less than one in two of the normally-hearing controls. At this intensity, the mean SP attenuation reached a reduction of 16% by the end of the stimulus sequence, thus proving significantly smaller than the CAP attenuation.

Since the *OTOF* children's responses to the high-rate click sequence (from the second to the eleventh click) showed different thresholds across ears, the amplitudes of the ECochG waveforms at intensities from 90 to 70 dB SPL were pooled together and were averaged at each click position (Fig. 8B, filled circles). We found that the mean attenuation in amplitude of the ECochG potentials during adaptation in children carrying *OTOF* mutations closely followed the mean CAP amplitude reduction calculated for normally-hearing controls in the range of intensities from 90 to 70 dB SPL. Moreover, while the duration of the normal controls' cochlear potentials did not change at the high stimulus rate, in the four *OTOF* children showing adaptation of the ECochG responses the duration of the prolonged ECochG waveforms dropped to control values after adaptation (Fig. 8C).

The changes found in the *OTOF* children, in both amplitude and duration of the ECochG responses, point to a neural rather than a receptor origin of the prolonged negative potentials. These prolonged responses are likely to result from the sum of small EPSPs arising in the terminal dendrites, which have an abnormal morphology and are dispersed in time as a consequence of the impaired multivesicle release. They seem similar to the dendritic responses recorded by Sellick et al. (2003) from the scala tympani of guinea pigs after blocking neural spiking in the terminal dendrites of auditory nerve fibers. These abnormal EPSPs only occasionally reach the threshold for triggering action potentials in some *OTOF* patients, which result in high-threshold CAPs superimposed on the prolonged responses. The impaired multivesicular release is therefore likely to result in a lower synaptic efficiency with a lesser probability of synchronized neural spiking and a reduced signaling to the auditory brainstem pathways in comparison with normal hearing. As a consequence, the behavioral thresholds appear considerably higher than the threshold of the prolonged potentials.

The adaptation pattern identified in the two *OTOF* children without prolonged potentials deviated considerably from the behavior seen in all the other patients. High stimulation rates induced no change in amplitude or duration of ECochG responses after adaptation (Fig. 8A, lower trace), consistently with their receptor generation. This adaptation pattern does not seem to correlate with a specific genotype because it was only seen in one of three affected siblings.

The ECochG results collected in the *OTOF* children are substantially consistent with findings in animal models of otoferlin-related hearing disorders. In the pachanga mouse DFNB9 model of human deafness the ECochG potentials only showed the SP component in response to tone-burst stimulation, suggesting that IHC activation was not followed by any generation of graded post-synaptic potentials. A small negative response, potentially representing a neural response, was nonetheless identified at high intensity (Pangršič et al., 2010). Moreover, high-threshold ABRs have been recorded in otoferlin-deficient mice (Roux et al., 2006), consistently with the activation of auditory brainstem pathways and the preservation of some residual hearing at high stimulus intensity.

Taken together, the findings obtained in patients with otoferlin-related ribbon synaptic disorders indicate that the impaired multivesicular release is not followed by auditory nerve fiber activation or, alternatively, it may result in an abnormal generation of EPSPs in auditory nerve fibers, with a consequent impairment of spike generation. These graded potentials are only occasionally followed by a synchronized electrical activity resulting in high-threshold CAPs. In other words, the impaired multivesicular release in otoferlin-related disorders represents the mechanism underlying the hearing dysfunction, but the magnitude of the resulting effects seems to be variable, ranging from mild hearing loss and slight speech perception impairment to profound deafness with some residual hearing.

6. Cochlear implantation

The benefits of cochlear implantation for improving speech perception in patients with auditory neuropathy depend on the site and severity of the damage involved. Electrical stimulation with a cochlear implant has proved to be effective in restoring speech perception in patients with post-synaptic AN due to *OPA1* mutations (Santarelli et al., 2015), and in AN related to other acquired disorders such as systemic sclerosis (Santarelli et al., 2006), while variable results have been obtained in AN associated with neurological disorders such as Friedreich's disease (Frewin et al., 2013; Miyamoto et al., 2000).

A positive outcome of using implants has already been reported in a few children with *OTOF* gene mutations (Chiu et al., 1010; Rouillon et al., 2006; Runge et al., 2013). Similar findings have been obtained in the patients reviewed in the present study, who all underwent unilateral cochlear implantation. Six of these children were implanted and subsequently followed up at our Department. Table 1 shows each patient's age at implant, the implanted ear and the type of device. CT and MRI scans of the head and ear were normal. All patients received the cochlear implant within six months of our first assessment, except for subject #2, who underwent cochlear implantation at the age of 4 because the parents had previously refused the procedure (Table 1).

All *OTOF* children showed a remarkable improvement in hearing sensitivity within three months of cochlear implant use. Their mean aided thresholds, measured in the free field with patients wearing their speech processor, fell within the estimated intensity range of conversational speech (Fig. 4).

The speech perception scores obtained in an open-set recognition test, administered to each child at an appropriate age, are given in Table 1. The tests were administered after using the cochlear implant for 1–1.5 years, when the children were at least at a minimum age of 3 years. The speech material consisted of disyllabic words in digital anechoic recordings made by a native Italian

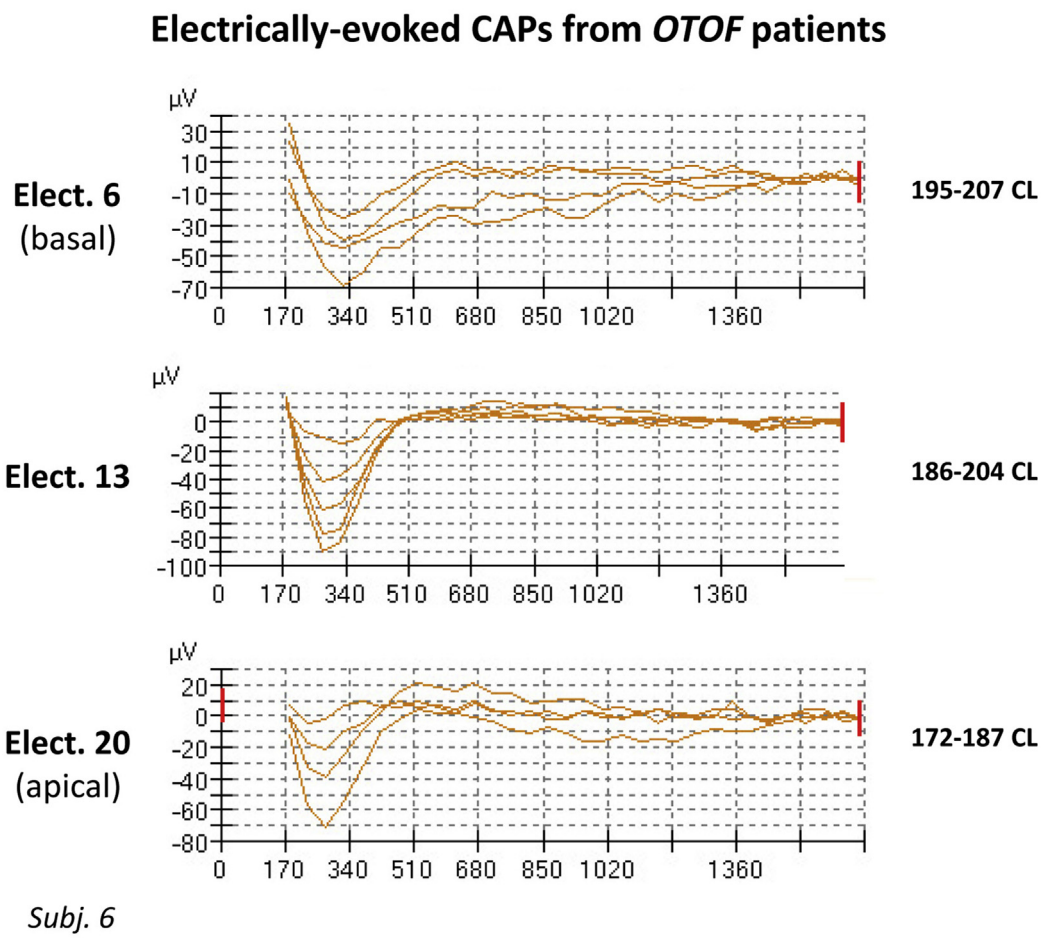

Fig. 9. Electrically-evoked compound action potentials (e-CAPs) from an implanted child (subject #6) carrying *OTOF* mutations (Nucleus C124RE with Freedom processor). The waveforms recorded at increasing stimulation intensities are shown for three different electrode locations. E-CAPs with typical morphology were recorded at each electrode location.

female speaker, which were presented in the free field at an intensity of 70 dB(A). The disyllabic words were obtained from an Italian adaptation (Arslan et al., 1997) of the word lists in the Northwestern University-Children's Perception of Speech (NU-CHIPs) tool (Elliot and Katz, 1980).

All the children reached speech perception scores of 90–100%. Their language development was also in line with the language skills of their peers with cochlear implants whose deafness was related to causes other than *OTOF* mutations.

Unlike patients with post-synaptic AN (Santarelli et al., 2015), the implanted children with ribbon synaptic disorders due to otoferlin dysfunction showed electrically-evoked auditory nerve responses (electrically-evoked compound action potentials, e-CAPs) obtained through the cochlear implant. Fig. 9 shows an example of the e-CAPs recorded at several electrode locations in a child with *OTOF* mutations (subj. #6). Increasing stimulation levels resulted in a higher amplitude and a slight decrease in the latency of the electrically-evoked neural responses. These results are consistent with a preserved auditory nerve fiber excitation and conduction in *OTOF*-related hearing disorders. Since exocytosis is reduced but not abolished in cases of abnormal otoferlin function (Pangršič et al., 2010; Roux et al., 2006), the persistence of some neurotransmitter release in the synaptic cleft may prevent the auditory nerve fiber degeneration believed to occur in other forms of congenital deafness due to hair cell loss (Shepherd and Javel, 1997).

7. Conclusion

Ribbon synaptic disorders relating to otoferlin dysfunction result in abnormal glutamate release in the synaptic cleft. The auditory nerve terminals are either not activated or they generate small EPSPs, which only occasionally trigger synchronized nerve spiking at high stimulation intensities. These local, graded responses are identifiable as prolonged potentials in ECochG recordings. This electrophysiological pattern is consistent with a limited synaptic efficiency and results in variable degrees of hearing loss.

Cochlear implants restore hearing sensitivity and speech perception. Recordings of electrically-evoked neural responses through the cochlear implant point to a preserved auditory nerve function. Based on these findings, the outcome of cochlear implantation in patients with presynaptic AN due to *OTOF* mutations can be expected to be invariably successful.

Acknowledgments

We are greatly indebted to all patients and their families for participating in our study. We are grateful to Fabio Saccomandi who wrote the software for data acquisition and analysis. We also thank nurses Alessia Musig and Tiziana Gavagnin for collecting the blood samples for genetic analysis, and Dr Manuela Spagnol for managing the classification and delivery of blood samples.

References

Arslan, E., Genovese, E., Orzan, E., Turrini, M., 1997. Valutazione Della Percezione Verbale Nel Bambino Ipoacusico. Ecumenica, Roma.

Artières, F., Vieu, A., Mondain, M., Uziel, A., Venail, F., 2009. Impact of early cochlear implantation on the linguistic development of the deaf child. Otol. Neurotol. 30, 736–742.

Bae, S.H., Baek, J.I., Lee, J.D., Song, M.H., Kwon, T.J., Oh, S.K., Jeong, J.Y., Choi, J.Y., Lee, K.Y., Kim, U.K., 2013. Genetic analysis of auditory neuropathy spectrum disorder in the Korean population. Gene 522, 65–69.

Berlin, C.I., Hood, L.J., Morlet, T., Wilensky, D., Li, L., Mattingly, K.R., Taylor-Jeanfreau, J., Keats, B.J., John, P.S., Montgomery, E., Shallop, J.K., Russell, B.A., Frisch, S.A., 2010. Multi-site diagnosis and management of 260 patients with auditory neuropathy/dys-synchrony (auditory neuropathy spectrum disorder). Int. J. Audiol. 49, 30–43.

Boothroyd, A., 2008. The acoustic speech signal. In: Madell, J.R., Flexer, C. (Eds.), Pediatric Audiology: Diagnosis, Technology, and Management. Thieme, New York, pp. 159–167.

Buran, B.N., Strenzke, N., Neef, A., Gundelfinger, E.D., Moser, T., Liberman, M.C., 2010. Onset coding is degraded in auditory nerve fibers from mutant mice lacking synaptic ribbons. J. Neurosci. 30, 7587–7597.

Chiu, Y.H., Wu, C.C., Lu, Y.C., Chen, P.J., Lee, W.Y., Liu, A.Y., Hsu, C.J., 2010. Mutations in the OTOF gene in Taiwanese patients with auditory neuropathy. Audiol. Neurootol. 15, 364–374.

Choi, B.Y., Ahmed, Z.M., Riazuddin, S., Bhinder, M.A., Shahzad, M., Husnain, T., Riazuddin, S., Griffith, A.J., Friedman, T.B., 2009. Identities and frequencies of mutations of the otoferlin gene (OTOF) causing DFNB9 deafness in Pakistan. Clin. Genet. 75, 237–243.

Dallos, P., Cheatham, M.A., 1976. Production of cochlear potentials by inner and outer hair cells. J. Acoust. Soc. Am. 60, 510–512.

Duman, D., Sirmaci, A., Cengiz, F.B., Ozdag, H., Tekin, M., 2011. Screening of 38 genes identifies mutations in 62% of families with nonsyndromic deafness in Turkey. Genet. Test. Mol. Biomarkers 15, 29–33.

Duncker, S.V., Franz, C., Kuhn, S., Schulte, U., Campanelli, D., Brandt, N., Hirt, B., Fakler, B., Blin, N., Ruth, P., Engel, J., Marcotti, W., Zimmermann, U., Knipper, M., 2013. Otoferlin couples to clathrin-mediated endocytosis in mature cochlear inner hair cells. J. Neurosci. 33, 9508–9519.

Durrant, J.D., Wang, J., Ding, D., Salvi, R., 1998. Are inner or outer hair cells the source of summating potentials recorded from the round window? J. Acoust. Soc. Am. 104, 370–377.

Eggermont, J.J., 1976. Electrocochleography. In: Keidel, W.D., Neff, W.D. (Eds.), Handbook of Sensory Physiology, Auditory System. Springer, New York, pp. 625–706.

Elberling, C., 1976. Simulation of cochlear action potentials recorded from the ear canal in man. In: Ruben, R.J., Elberling, C., Salomon, G. (Eds.), Electrocochleography. University Park Press, Baltimore, pp. 151–168.

Elliot, L.L., Katz, D.R., 1980. Development of a New Children's Test of Speech Discrimination. Auditec, Saint Louis.

Frewin, B., Chung, M., Donnelly, N., 2013. Bilateral cochlear implantation in Friedreich's ataxia: a case study. Cochlear Implants Int. 14, 287–290.

Geers, A.E., Moog, J.S., 1991. Evaluating the benefits of cochlear implants in an education setting. Am. J. Otol. (Suppl. 12), 116–125.

Glowatzki, E., Fuchs, P.A., 2002. Transmitter release at the hair cell ribbon synapse. Nat. Neurosci. 5, 147–154.

Hossain, W.A., Antic, S.D., Yang, Y., Rasband, M.N., Morest, D.K., 2005. Where is the spike generator of the cochlear nerve? Voltage-gated sodium channels in the mouse cochlea. J. Neurosci. 25, 6857–6868.

Hutchin, T., Coy, N.N., Conlon, H., Telford, E., Bromelow, K., Blaydon, D., Taylor, G., Coghill, E., Brown, S., Trembath, R., Liu, X.Z., Bitner-Glindzicz, M., Mueller, R., 2005. Assessment of the genetic causes of recessive childhood non-syndromic deafness in the UK - implications for genetic testing. Clin. Genet. 68, 506–512.

Iwasa, Y., Nishio, S.Y., Yoshimura, H., Kanda, Y., Kumakawa, K., Abe, S., Naito, Y., Nagai, K., Usami, S., 2013. OTOF mutation screening in Japanese severe to profound recessive hearing loss patients. BMC Med. Genet. 14, 95.

Jin, Y.J., Park, J., Kim, A.R., Rah, Y.C., Choi, B.Y., 2014. Identification of a novel splice site variant of OTOF in the Korean nonsyndromic hearing loss population with low prevalence of the OTOF mutations. Int. J. Pediatr. Otorhinolaryngol. 78, 1030–1035.

Johnson, C.P., Chapman, E.R., 2010. Otoferlin is a calcium sensor that directly regulates SNARE-mediated membrane fusion. J. Cell Biol. 191, 187–197.

Mahdieh, N., Shirkavand, A., Rabbani, B., Tekin, M., Akbari, B., Akbari, M.T., Zeinali, S., 2012. Screening of OTOF mutations in Iran: a novel mutation and review. Int. J. Pediatr. Otorhinolaryngol. 76, 1610–1615.

Marlin, S., Feldmann, D., Nguyen, Y., Rouillon, I., Loundon, N., Jonard, L., Bonnet, C., Couderc, R., Garabedian, E.N., Petit, C., Denoyelle, F., 2010. Temperature-sensitive auditory neuropathy associated with an otoferlin mutation: deafening fever! Biochem. Biophys. Res. Commun. 394, 737–742.

Matsunaga, T., Mutai, H., Kunishima, S., Namba, K., Morimoto, N., Shinjo, Y., Arimoto, Y., Kataoka, Y., Shintani, T., Morita, N., Sugiuchi, T., Masuda, S., Nakano, A., Taiji, H., Kaga, K., 2012. A prevalent founder mutation and genotype-phenotype correlations of OTOF in Japanese patients with auditory neuropathy. Clin. Genet. 82, 425–432.

McMahon, C.M., Patuzzi, R.B., Gibson, W.P.R., Sanli, H., 2008. Frequency-specific electrocochleography indicates that presynaptic and postsynaptic mechanisms of auditory neuropathy exist. Ear Hear 29, 314–325.

Miyamoto, R.T., Kirk, K.I., Renshaw, J., Hussain, D., Seghal, S.T., 2000. Cochlear implantation in auditory neuropathy. Adv. Otorhinolaryngol. 57, 160–161.

Moser, T., Neef, A., Khimich, D., 2006. Mechanisms underlying the temporal precision of sound coding at the inner hair cell ribbon synapse. J. Physiol. 576, 55–62.

Nicholas, J.G., Geers, A.E., 2007. Will they catch up? The role of age at cochlear implantation in the spoken language development of children with severe to profound hearing loss. J. Speech Lang. Hear. Res. 50, 1048–1062.

Pangršič, T., Lasarow, L., Reuter, K., Takago, H., Schwander, M., Riedel, D., Frank, T., Tarantino, L.M., Bailey, J.S., Strenzke, N., Brose, N., Müller, U., Reisinger, E., Moser, T., 2010. Hearing requires otoferlin-dependent efficient replenishment of synaptic vesicles in hair cells. Nat. Neurosci. 13, 869–876.

Pangršič, T., Reisinger, E., Moser, T., 2012. Otoferlin: a multi-C2 domain protein essential for hearing. Trends Neurosci. 35, 671–680.

Ramakrishnan, N.A., Drescher, M.J., Drescher, D.G., 2009. Direct interaction of otoferlin with syntaxin 1A, SNAP-25, and the L-type voltage-gated calcium channel Cav1.3. J. Biol. Chem. 284, 1364–1372.

Rodríguez-Ballesteros, M., del Castillo, F.J., Martín, Y., Moreno-Pelayo, M.A., Morera, C., Prieto, F., Marco, J., Morant, A., Gallo-Terán, J., Morales-Angulo, C., Navas, C., Trinidad, G., Tapia, M.C., Moreno, F., del Castillo, I., 2003. Auditory neuropathy in patients carrying mutations in the otoferlin gene (OTOF). Hum. Mut. 22, 451–456.

Rodríguez-Ballesteros, M., Reynoso, R., Olarte, M., Villamar, M., Morera, C., Santarelli, R., Arslan, E., Medá, C., Curet, C., Völter, C., Sainz-Quevedo, M., Castorina, P., Ambrosetti, U., Berrettini, S., Frei, K., Tedín, S., Smith, J., Cruz Tapia, M., Cavallé, L., Gelvez, N., Primignani, P., Gómez-Rosas, E., Martín, M., Moreno-Pelayo, M.A., Tamayo, M., Moreno-Barral, J., Moreno, F., del Castillo, I., 2008. A multicenter study on the prevalence and spectrum of mutations in the otoferlin gene (OTOF) in subjects with nonsyndromic hearing impairment and auditory neuropathy. Hum. Mut. 29, 823–831.

Romanos, J., Kimura, L., Fávero, M.L., Izarra, F.A., de Mello Auricchio, M.T., Batissoco, A.C., Lezirovitz, K., Abreu-Silva, R.S., Mingroni-Netto, R.C., 2009. Novel OTOF mutations in Brazilian patients with auditory neuropathy. J. Hum. Genet. 54, 382–385.

Rouillon, I., Marcolla, A., Roux, I., Marlin, S., Feldmann, D., Couderc, R., Jonard, L., Petit, C., Denoyelle, F., Garabédian, E.N., Loundon, N., 2006. Results of cochlear implantation in two children with mutations in the OTOF gene. Int. J. Pediatr. Otorhinolaryngol. 70, 689–696.

Roux, I., Safieddine, S., Nouvian, R., Grati, M., Simmler, M.C., Bahloul, A., Perfettini, I., Le Gall, M., Rostaing, P., Hamard, G., Triller, A., Avan, P., Moser, T., Petit, C., 2006. Otoferlin, defective in a human deafness form, is essential for exocytosis at the auditory ribbon synapse. Cell 127, 277–289.

Runge, C.L., Erbe, C.B., McNally, M.T., Van Dusen, C., Friedland, D.R., Kwitek, A.E., Kerschner, J.E., 2013. A novel otoferlin splice-site mutation in siblings with auditory neuropathy spectrum disorder. Audiol. Neurootol. 18, 374–382.

Santarelli, R., 2010. Information from cochlear potentials and genetic mutations helps localize the lesion site in auditory neuropathy. Genome Med. 2, 91.

Santarelli, R., Arslan, E., 2002. Electrocochleography in auditory neuropathy. Hear. Res. 170, 32–47.

Santarelli, R., Arslan, E., 2013. Electrocochleography. In: Celesia, G.G. (Ed.), Disorders of Peripheral and Central Auditory Processing, Handbook of Clinical Neurophysiology. Elsevier, Amsterdam, pp. 83–113.

Santarelli, R., Arslan, E., 2015. Electrocochleography. In: Katz, J., Chasin, M., English, K., Hood, L., Tillery, K.L. (Eds.), Handbook of Clinical Audiology, seventh ed. Wolters Kluwer, Philadelphia, pp. 207–230.

Santarelli, R., Scimemi, P., Dal Monte, E., Genovese, E., Arslan, E., 2006. Auditory neuropathy in systemic sclerosis: a speech perception and evoked potential study before and after cochlear implantation. Eur. Arch. Otorhinolaryngol. 263, 809–815.

Santarelli, R., Starr, A., Michalewski, H.J., Arslan, E., 2008. Neural and receptor cochlear potentials obtained by transtympanic electrocochleography in auditory neuropathy. Clin. Neurophysiol. 119, 1028–1041.

Santarelli, R., del Castillo, I., Rodríguez-Ballesteros, M., Scimemi, P., Cama, E., Arslan, E., Starr, A., 2009. Abnormal cochlear potentials from deaf patients with mutations in the otoferlin gene. J. Assoc. Res. Otolaryngol. 10, 545–556.

Santarelli, R., Rossi, R., Arslan, E., 2013a. Assistive devices for patients with auditory neuropathy: hearing aid use. Semin. Hear 34, 51–64.

Santarelli, R., del Castillo, I., Starr, A., 2013b. Auditory neuropathies and electrocochleography. Hear. Balance Communic 11, 130–137.

Santarelli, R., Rossi, R., Scimemi, P., Cama, E., Valentino, M.L., La Morgia, C., Caporali, L., Liguori, R., Magnavita, V., Monteleone, A., Biscaro, A., Arslan, E., Carelli, V., 2015. OPA1-related auditory neuropathy: site of lesion and outcome of cochlear implantation. Brain 138, 563–576.

Sellick, P., Patuzzi, R., Robertson, D., 2003. Primary afferent and cochlear nucleus contributions to extracellular potentials during tone-bursts. Hear. Res. 176, 42–58.

Shepherd, R.K., Javel, E., 1997. Electrical stimulation of the auditory nerve. I. Correlation of physiological responses with cochlear status. Hear. Res. 108, 112–144.

Starr, A., Picton, T.W., Sininger, Y., Hood, L.J., Berlin, C.I., 1996. Auditory neuropathy. Brain 119, 741–753.

Starr, A., Sininger, Y., Winter, M., Derebery, M.J., Oba, S., Michalewski, H.J., 1998. Transient deafness due to temperature-sensitive auditory neuropathy. Ear Hear 19, 169–179.

Starr, A., Sininger, Y.S., Pratt, H., 2000. The varieties of auditory neuropathy. J. Basic Clin. Physiol. Pharmacol. 11, 215–230.
Starr, A., Sininger, Y., Nguyen, T., Michalewski, H.J., Oba, S., Abdala, C., 2001. Cochlear receptor (microphonic and summating potentials, otoacoustic emissions) and auditory pathway (auditory brain stem potentials) activity in auditory neuropathy. Ear Hear 22, 91–99.
Starr, A., Michalewski, H.J., Zeng, F.G., Fujikawa-Brooks, S., Linthicum, F., Kim, C.S., Winnier, D., Keats, B., 2003. Pathology and physiology of auditory neuropathy with a novel mutation in the MPZ gene (Tyr145->Ser). Brain 126, 1604–1619.
Starr, A., Isaacson, B., Michalewski, H.J., Zeng, F.G., Kong, Y.Y., Beale, P., Paulson, G.W., Keats, B.J., Lesperance, M.M., 2004. A dominantly inherited progressive deafness affecting distal auditory nerve and hair cells. J. Assoc. Res. Otolaryngol. 5, 411–426.
Starr, A., Zeng, F.G., Michalewski, H.J., Moser, T., 2008. Perspectives on auditory neuropathy: disorders of inner hair cell, auditory nerve, and their synapse. In: Dallos, P., Oertel, D. (Eds.), The Senses: a Comprehensive Reference, Audition, vol. 3. Elsevier, Amsterdam, pp. 397–412.
Varga, R., Kelley, P.M., Keats, B.J., Starr, A., Leal, S.M., Cohn, E., Kimberling, W.J., 2003. Non-syndromic recessive auditory neuropathy is the result of mutations in the otoferlin (OTOF) gene. J. Med. Genet. 40, 45–50.
Varga, R., Avenarius, M.R., Kelley, P.M., Keats, B.J., Berlin, C.I., Hood, L.J., Morlet, T.G., Brashears, S.M., Starr, A., Cohn, E.S., Smith, R.J., Kimberling, W.J., 2006. OTOF mutations revealed by genetic analysis of hearing loss families including a potential temperature sensitive auditory neuropathy allele. J. Med. Genet. 43, 576–581.
Wang, D.Y., Wang, Y.C., Weil, D., Zhao, Y.L., Rao, S.Q., Zong, L., Ji, Y.B., Liu, Q., Li, J.Q., Yang, H.M., Shen, Y., Benedict-Alderfer, C., Zheng, Q.Y., Petit, C., Wang, Q.J., 2010. Screening mutations of OTOF gene in Chinese patients with auditory neuropathy, including a familial case of temperature-sensitive auditory neuropathy. BMC Med. Genet. 11, 79.
Wynne, D.P., Zeng, F.G., Bhatt, S., Michalewski, H.J., Dimitrijevic, A., Starr, A., 2013. Loudness adaptation accompanying ribbon synapse and auditory nerve disorders. Brain 136, 1626–1638.
Yasunaga, S., Grati, M., Cohen-Salmon, M., El-Amraoui, A., Mustapha, M., Salem, N., El-Zir, E., Loiselet, J., Petit, C., 1999. A mutation in OTOF, encoding otoferlin, a FER-1-like protein, causes DFNB9, a nonsyndromic form of deafness. Nat. Genet. 21, 363–369.
Yasunaga, S., Grati, M., Chardenoux, S., Smith, T.N., Friedman, T.B., Lalwani, A.K., Wilcox, E.R., Petit, C., 2000. OTOF encodes multiple long and short isoforms: genetic evidence that the long ones underlie recessive deafness DFNB9. Am. J. Hum. Genet. 67, 591–600.
Zeng, F.G., Kong, Y.Y., Michalewski, H.J., Starr, A., 2005. Perceptual consequences of disrupted auditory nerve activity. J. Neurophysiol. 93, 3050–3063.